SAR INTERFEROMETRIC DATA INVERSION: A STUDY ABOUT NUMERICAL APPROACHES

G. Nunnari[(1)], G. Puglisi[(2)] , F. Guglielmino[(2)] and F. Accetta[(1)]
[(1)]Dipartimento di Ingegneria Elettrica, Elettronica e dei Sistemi, Università di Catania, Italy, gnunnari@diees.unict.it
[(2):]Istituto Nazionale di Geofisica e Vulcanologia, Sezione di Catania, Italy,puglisi-g@ct.ingv.it;

ABSTRACT
SAR interferometry is currently one of the most powerful techniques for observation of the Earth's surface, in particular for both topographical measurements of vast geographical areas and surface change measurements over a pre-defined time interval (Differential Radar Interferometry). The inversion problem considered in this paper consists of identifying the parameters of a ground deformation source by observing the changes it causes in SAR interferometric data. Investigations into the structural analysis of the mathematical model, show that the problem is an extremely nonlinear one. Hence the inversion solution cannot be obtained in closed form but it can be formulated as an optimization search problem. The search is tackled by using the Genetic Algorithms (GAs) approach since it guarantees against the problem of local minima. Synthetic data are first considered to study the accuracy of the inverse solution. Hence actual SAR data recorded during the recent 2001 Mt Etna eruption are taken into account for the inversion exercise. The results obtained are discussed also in comparison with the inversion of an independent set of GPS data.

1 GENERATION OF SAR SYNTHETIC DATA

The model refers to volcanic areas such as *Mt. Etna* (Sicily – Italy), where a number of eruptions have their origin in dikes opening from a certain depth toward the surface. These phenomena are accompanied by variations in geophysical magnitudes, especially ground deformations and anomalies in the magnetic and gravity fields. The considered geophysical phenomena may be observed when a crack opens up due to the intrusion of magma. Compared to the real situation, the Okada source model (Fig. 1) is of course greatly simplified.

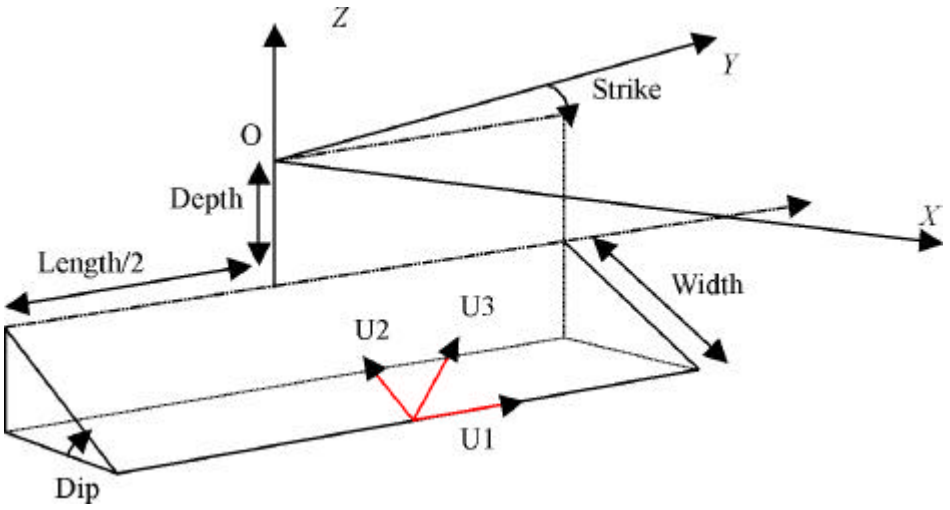

Fig. 1: The Okada dislocation source: it models a fault or dyke in a homogeneous and isotropic elastic half-space. Depth is the distance between the origin O and the upper edge of the source; Strike is the orientation of the source with respect to the North; Dip (hereafter δ) is angle of the dislocation plane with respect the horizontal plane; Length and Width are the length and width of the source respectively; U_1, U_2 and U_3 are the Strike-slip, Dip-slip and Tensile dislocation components respectively.

A detailed analysis of the whole set of analytical expressions due to an Okada type source is beyond the scope of this paper. Here only the components u_x, u_y, u_z of the measured deformation vector due to a tensile displacement are given (Eqs. 1-4) in order to show the high degree of non-linearity with respect to the model parameters:

$$\begin{cases} u_x = \dfrac{U_3}{2p}\left[\dfrac{q^2}{R(R+h)} - I_3 \sin^2 d\right] \\ u_y = \dfrac{U_3}{2p}\left[\dfrac{-\tilde{d}q}{R(R+x)} - \sin d\left\{\dfrac{xq}{R(R+h)} - \tan^{-1}\dfrac{xh}{qR}\right\} - I_1 \sin^2 d\right] \\ u_z = \dfrac{U_3}{2p}\left[\dfrac{\tilde{y}q}{R(R+x)} + \cos d\left\{\dfrac{xq}{R(R+h)} - \tan^{-1}\dfrac{xh}{qR}\right\} - I_5 \sin^2 d\right] \end{cases} \quad (1)$$

where

$$\begin{cases} p = y\cos d + d\sin d \\ q = y\sin d - d\cos d \\ \tilde{y} = h\cos d + q\sin d \\ \tilde{d} = h\sin d - q\cos d \\ R^2 = x^2 + h^2 + q^2 = x^2 + \tilde{y}^2 + \tilde{d}^2 \\ X^2 = x^2 + q^2 \end{cases} \quad (2)$$

being

$$\begin{cases} I_1 = \dfrac{m}{l+m}\left[\dfrac{-1}{\cos d}\dfrac{x}{R+\tilde{d}}\right] - \dfrac{\sin d}{\cos d} I_5 \\ I_2 = \dfrac{m}{l+m}\left[-\ln(R+h)\right] - I_3 \\ I_3 = \dfrac{m}{l+m}\left[\dfrac{1}{\cos d}\dfrac{\tilde{y}}{R+\tilde{d}} - \ln(R+h)\right] + \dfrac{\sin d}{\cos d} I_4 \\ I_4 = \dfrac{m}{l+m}\dfrac{1}{\cos d}\left[\ln(R+\tilde{d}) - \ln(R+h)\sin d\right] \\ I_5 = \dfrac{m}{l+m}\dfrac{2}{\cos d}\tan^{-1}\dfrac{h(X+q\cos d) + X(R+X)\sin d}{x(R+X)\cos d} \end{cases} \quad (3)$$

if $\cos d \neq 0$, and

$$\begin{cases} I_1 = -\dfrac{m}{2(l+m)}\dfrac{xq}{\left(R+\tilde{d}\right)^2} \\ I_3 = \dfrac{m}{2(l+m)}\left[\dfrac{h}{R+\tilde{d}} + \dfrac{\tilde{y}q}{\left(R+\tilde{d}\right)^2} - \ln(R+h)\right] \\ I_4 = -\dfrac{m}{l+m}\dfrac{q}{R+\tilde{d}} \\ I_5 = -\dfrac{m}{l+m}\dfrac{x\sin d}{R+\tilde{d}} \end{cases} \quad (4)$$

if $\cos d = 0$ (i.e. if the dislocation plane is vertical).

In these equations, (*x*, *y*, *z*) and (*?*, *?*, *q*) are coordinates of appropriate reference systems; *R*, $\tilde{d}$ and $\tilde{y}$ scalar quantities; the symbol "||" represents Chinnery's notation. Let us indicate by P_i be a generic point on the XY (i.e. the plane where the deformations are measured). Once u_x, u_y, u_z are computed, the components U_X, U_Y, U_Z of the deformation vector *U* at P_i referred to the *O(X,Y,Z)* reference system can be obtained as follows:

$$\begin{cases} U_X = u_x \sin s - u_y \cos s \\ U_Y = u_x \cos s + u_y \sin s \\ U_Z = u_z \end{cases} \qquad (5)$$

where *s* is the *Strike* angle. In order to be able to generate a synthetic interferogram it is necessary to compute the projection of the deformation components U_X, U_Y, and U_Z along the direction of the satellite view. To this end, let us indicate by ***?*** be the vector of the direction cosines that defines the satellite view angle with respect to the *O(X,Y,Z)* reference system. Hence the searched projection is

$$U_r = r \cdot U = r_X U_X + r_Y U_Y + r_Z U_Z \qquad (6)$$

The quantity $U_?$ must be scaled into the interval *0-2p* to calculate the traditional *fringes* that characterize an interferogram, by using the relation

$$\overline{U}_r = \frac{2p}{l} frac\left(\frac{U_r}{l}\right) \qquad (7)$$

where *?* is the principal wave length emitted by the satellite antenna, that is $28*10^{-3}$ *m* in the case of *ERS-2*, and *frac()* is the fractionary part.

Examples of ground deformations and synthetic interferogram due to an Okada source whose parameters are given in Tab. I are represented in Fig. 2.

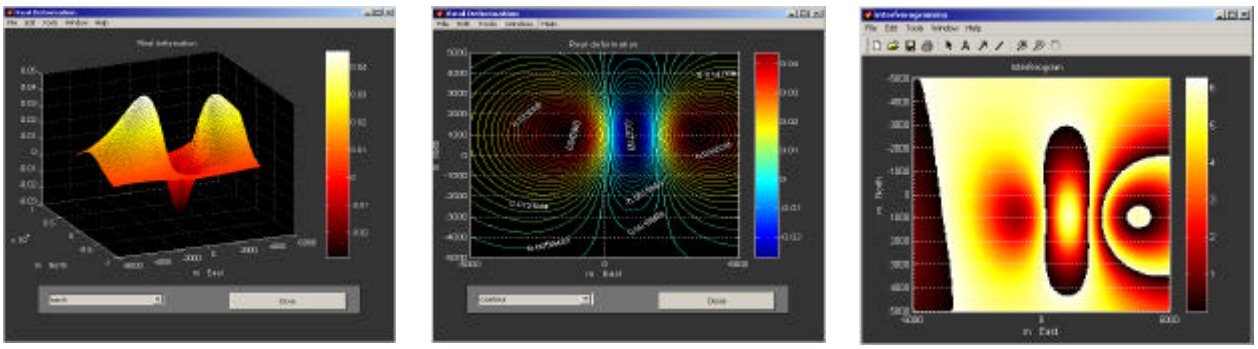

Fig. 2: a) Ground deformation, b) contour , c) SAR interferogram.

Tab I: parameters of the Okada source corresponding to the plots given in Fig. 2

Dip (°)	**Strike** (°)	**Length** (Km)	**Width** (Km)	**U1** (m)	**U2** (m)	**U3** (m)	**Depth** (Km)	**X_S** (Km)	**Y_S** (Km)
89	180	1	2	0	0	3	2	1	1

2 Inverse Modelling

GAs algorithm is currently one of the most powerful methods for the solution of non-linear optimization problems. The reason for using GAs is that they are capable of finding the global minimum of a function with many variables, thereby overcoming the limitation of typical gradient-based techniques. The experimental framework was formulated as follows. A regular grid, 10 by 10 km wide and centered on the summit volcano area, was defined and ground deformation were computed at the vertices of the grid by using an appropriate software tool based on Okada model. One hundred model sources uniformly distributed in the space of parameters were separately considered, hypothesizing a grid consisting of 21x21 vertices (i.e. 441 measuring points). No noise was added to the synthetic generated data. The cost function was defined according to expression (8), where N represents the number of measuring points while O_i and P_i indicate the expected and simulated values respectively.

$$J = \sum_{i=1}^{N} \sqrt{\left(O_i - P_i \right)^2} \qquad (8)$$

Simulation were also carried out assuming as cost function the *fitness*, defined as:

$$J = \frac{\sum_{i=1}^{N} (P_i - O_i)^2}{\sum_{i=1}^{N} (|P_i - \overline{O}| + |O_i - \overline{O}|)^2} \qquad (9)$$

In order to evaluate the performance of the considered inverse modelling approach an appropriate number of performance indexes have been evaluated, including the Bias (10), the *RMSE* (Root Square Mean Error) (11), the *MAE* (Mean Absolute Error) (12) that give estimates of the average error, the NMAE% (Percentage Normalised MAE) (13) and the index of agreement d (14) which is a bounded relative measure capable of measuring the degree to which predictions are error-free.

$$Bias: \quad \frac{1}{N} \sum_{i=1}^{N} (P_i - O_i) \qquad (10)$$

$$RMSE: \quad \sqrt{\frac{1}{N} \sum_{i=1}^{N} (P_i - O_i)^2} \qquad (11)$$

$$MAE: \quad \frac{1}{N} \sum_{i=1}^{N} |P_i - O_i| \qquad (12)$$

$$NMAE\% = \frac{100}{(N \cdot Range)} \sum_{i=1}^{N} |P_i - O_i| \qquad (13)$$

$$d: \quad 1 - \frac{\sum_{i=1}^{N} (P_i - O_i)^2}{\sum_{i=1}^{N} (|P_i - \bar{O}| + |O_i - \bar{O}|)^2} \qquad (14)$$

In the expressions above, the over bar indicates the mean value while the suffix i represents the generic value. The results obtained are shown in the following Table II. It can be seen that all the model parameters are estimated with a NMAE% that is lower that 5% in case of free-noise data. In more detail the source coordinates the Dip and Strike angles, the Length and Width of the fault and the opening dislocation component U_3 are obtained with a NMAE% lower than 1%, the coordinates X_s and Y_s *exhibits* NMAE% lower than 2% and finally the Depth and the U_1 and U_2 dislocation components exhibits NMAE% lower than 5%. No appreciable differences were observed by using expression (7) as cost function. The results obtained show that the inverse problem considered can be solved with high accuracy in case of free noise synthetic data, in the hypothesis that the deformation is due to a single dislocation.

Table II – Performance Indices of the GA inverse modelling approach

Parameter	*Bias*	*MAE*	*RMSE*	*NMAE%*	*d*
Dip	-0.2533	0.2533	0.3136	0.2815	0.9999
Strike	-0.2435	0.2435	0.3215	0.0676	0.9997
Length	0.0177	0.0177	0.0247	0.2952	0.9965
Width	0.0027	0.0132	0.0155	0.3291	0.9978
U1	-0.0642	0.1390	0.1561	3.4742	0.9990
U2	0.1998	0.1998	0.2117	4.9946	0.9904
U3	-0.0048	0.0206	0.0210	0.5161	0.9972
Depth	0.1206	0.1206	0.1330	3.0139	0.9956
Xs	-0.1455	0.1355	0.1822	0.7275	0.9877
Ys	0.0178	0.2666	0.2831	1.3329	0.9994

3 Actual data inversion

In order to test the algorithm with actual data, we have considered a descending interferogram (Fig 3a) referring to image pair 15 Nov.2000 - 31 Oct. 2001 of Mt Etna area. The low quality of images suggested to use a resized area (Fig 3b) characterized by a high coherence. This allowed obtaining a good map of displacement vectors along the line of sight. As for the synthetic data inversion have considered the case of a tensile dislocation therefore the Strike and Dip dislocation components have been forced to be zero, while the remaining parameters were assumed free to be searched within their physical ranges. The search process was stopped when the index of agreement (6) and the fitness (7) (both assumed in the cost function to be minimized) approached the level of 99%. The results of the Genetic Algorithm search are shown in the first column of Table 3. The parameters of the dyke are consistent with geological evidences and with results reported in others papers concerning the 2001 Etna eruption such as [1]. To further validate the obtained results, the inversion of an independent set of GPS data, recorded during July-September 2001, was performed and the results of the search procedure are shown in the second column in Table III.

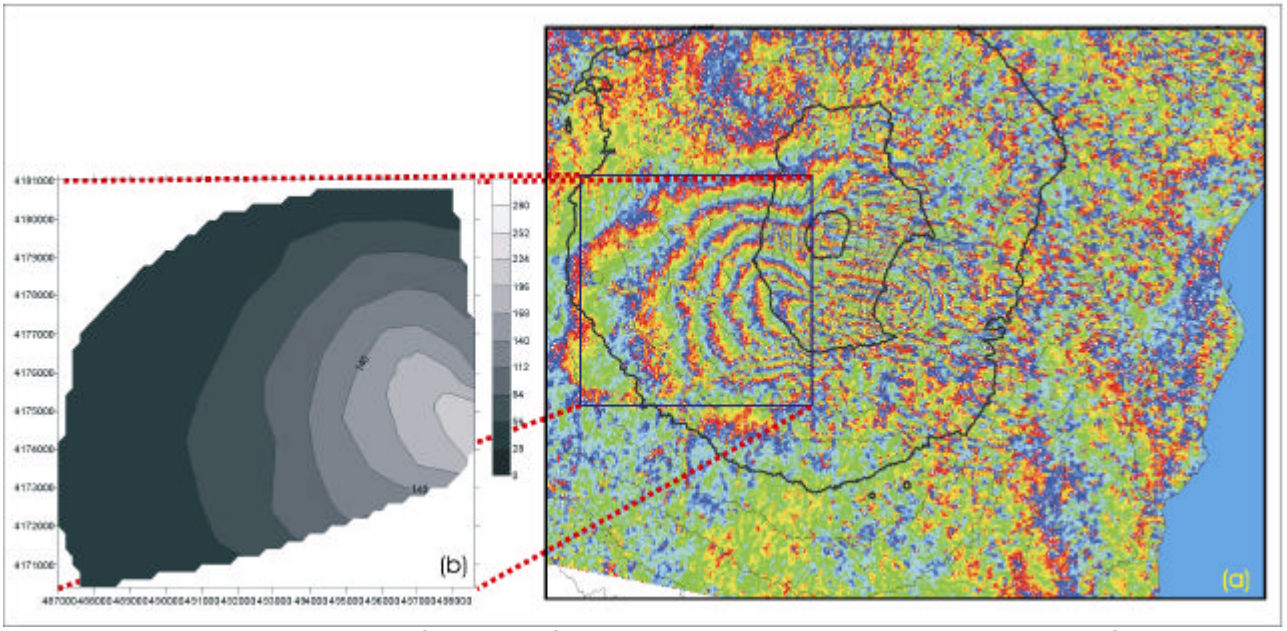

Fig 3: (a)Geocoded descending interferogram refers to image pair 15 Nov.2000_31 Oct. 2001 of Etna area and (b)geocoded LOS displacement(expressed in mm) map of resize area

Table III – Inversion results

	Inversion from SAR data	**Inversion from GPS data**
Lat. UTM (km)	500.77	500.65
Long UTM (km)	4176.275	4175.5
Azimuth °	1.3	3.4
Depth (km)	1.5 a.s.l.	1.6 a.s.l.
Length (km)	7.4	2.34
Width (km)	1.5	3.55
Dip °	89.9	89
U_3 (cm)	300.0	251.7

The comparison between SAR and GPS results shows a high agreement between the Latitude, Longitude, Azimuth, Depth, Dip and Opening parameters. On the other hand it is possible to observe a significant difference between the Length and Width parameters in the two considered cases. The authors have tried to interpret the differences concerning these two model parameters invoking the fact that SAR and GPS were recorded in different time intervals. Indeed SAR data refers to a time interval spanning from November 2000 to October 2001, while GPS data were recorded during July-September 2001. This means that probably SAR data reflects the presence of some different deformation episodes that however are less significant with respect the main dyke intrusion.

4 Conclusions

This paper has proposed a method for the nonlinear inversion of SAR interferometric data by using a GA optimisation algorithm. More specifically, it has dealt with the inversion of ground deformation data relating to magma-filled dikes in volcanic areas. Situations of this kind are very frequent in areas like that of Mt. Etna. The goodness of the inversion procedure has been assessed both using synthetic and real SAR data. The inversion of synthetic data has shown a high reliability of the proposed approach. Some further validation is still required dealing with real data due to the problem of multiple sources. To this end work is in progress. In particular we intend to perform the inversion of a SAR interferograms that were not available at the time of this study. Moreover we intend to use wrapped data instead of unwarepped ones in order to avoid possible ambiguities.

Acknowledgement

This work has been supported by the Italian GNV (Gruppo Nazionale per la Vulcanologia) under the coordinate project “Sviluppo ed Applicazione di Tecniche di Telerilevamento per il Monitoraggio dei Vulcani Attivi Italiani”. The ERS data were provided in the frame of the ERS AO3-359 project.

References

[1] Bonaccorso A., M. Aloisi, M. Mattia, 2002 ,Dike emplacement forerunning the Etna July 2001 eruption modelled through continuous tilt and GPS data, *Geophysical Research Letters*,29,13.
[2] Curlander J. C. and McDonough R. N., 1991, *Synthetic Aperture Radar, Systems & Signal Processing, Introduction to SAR*, J. Wiley & Sons Inc, New York.
[3] Lanari R., Fornaro G., Riccio D., Migliaccio M., Papathanassiou K. P., Moreira J. R., Schwäbisch M., Dutra L., Puglisi G., Franceschetti G., Coltelli M., 1996, Generation of Digital Elevation Models by Using SIR-C/X-SAR Multifrequency Two-Pass Interferometry: The Etna Case Study, IEEE Trans. on *Geoscience and Remote Sensing*, 34, 5, p. 1097-1114.
[4] Okada, Y., Surface deformation due to shear and tensile faults in a halfspace, 1985, *Bull. Seismol. Soc. Amer.*, vol. 75, p. 1135–1154.